metals

MDPI

Article

Tailoring the Microstructure of Laser-Additive-Manufactured Titanium Aluminide Alloys via In Situ Alloying and Parameter Variation

Igor Polozov *, Victoria Sokolova, Anna Gracheva and Anatoly Popovich

Institute of Mechanical Engineering, Materials, and Transport, Peter the Great St. Petersburg Polytechnic University (SPbPU), Polytechnicheskaya, 29, St. Petersburg 195251, Russia; sokolova_vv@spbstu.ru (V.S.); gracheva_am@spbstu.ru (A.G.); director@immet.spbstu.ru (A.P.)
* Correspondence: polozov_ia@spbsbtu.ru

Abstract: Titanium aluminide (TiAl) alloys have emerged as promising materials for high-temperature applications due to their unique combination of high-temperature strength, low density, and excellent oxidation resistance. However, the fabrication of TiAl alloys using conventional methods is challenging due to their high melting points and limited ductility. Selective laser melting (SLM), an additive manufacturing technique, offers a viable solution for producing TiAl alloys with intricate geometries and the potential for tailoring their microstructure. This study investigates the effect of in situ copper alloying and multiple laser scans on the microstructure and mechanical properties of TiAl-based alloys fabricated using SLM. The results demonstrate that copper alloying enhances the formation of the α_2-Ti_3Al phase, refines the microstructure, and improves the mechanical properties of TiAl alloys. Multiple laser scans allow for the creation of distinct microstructural regions within a single component, enabling the tailoring of properties that are suitable for specific operating conditions. The findings provide valuable insights into the fabrication and optimization of TiAl intermetallic alloys with diverse applications.

Keywords: titanium aluminide; additive manufacturing; in situ alloying; selective laser melting; Ti4822

Citation: Polozov, I.; Sokolova, V.; Gracheva, A.; Popovich, A. Tailoring the Microstructure of Laser-Additive-Manufactured Titanium Aluminide Alloys via In Situ Alloying and Parameter Variation. *Metals* **2023**, *13*, 1429. https://doi.org/10.3390/met13081429

Academic Editor: Andrea Di Schino

Received: 14 July 2023
Revised: 2 August 2023
Accepted: 8 August 2023
Published: 9 August 2023

1. Introduction

Titanium aluminide (TiAl) alloys have gained significant attention in recent years due to their exceptional combination of high-temperature strength, low density, and excellent oxidation resistance, making them promising materials for applications in the aerospace and automotive industries, among others [1–3]. However, the fabrication of TiAl intermetallic alloys poses significant challenges when using conventional manufacturing methods, primarily due to the materials' high melting points and limited ductility [4]. Selective laser melting (SLM), an additive manufacturing (AM) technique, offers a viable solution for producing TiAl alloys with intricate geometries and raises the possibility of tailoring their microstructures [5].

While the AM of intermetallic TiAl alloys has significant benefits, such as its ability to produce complex geometries with high precision, the fabrication of TiAl intermetallic alloys with SLM still poses significant challenges. The inherent characteristics of TiAl alloys, such as their high melting points and susceptibility to cracking, constitute obstacles to achieving the desired microstructures. To address these challenges, high-temperature substrate preheating is often employed to mitigate cracking issues during the SLM process [6,7].

One effective approach for enhancing the properties of TiAl-based alloys is alloying with other elements. The addition of specific alloying elements, such as niobium (Nb), vanadium (V), and chromium (Cr), has been shown to improve the mechanical strength, ductility, and high-temperature stability of TiAl alloys [4,8]. These alloying elements can

influence the materials' phase composition, grain refinement, and precipitation behavior, leading to enhanced properties and the improved performance of TiAl alloys in various applications. Additionally, small amounts of elements such as boron (B), zirconium (Zr), and silicon (Si) have been investigated in attempts to refine the microstructure of and promote the formation of desirable phases in TiAl alloys [9,10]. These elements can influence the grain boundary strength, precipitation kinetics, and overall microstructural stability, resulting in the improved mechanical properties, oxidation resistance, and creep resistance of TiAl alloys.

One approach to enhancing the microstructural characteristics and mechanical properties of TiAl alloys is through the utilization of in situ alloying. In situ alloying involves the introduction of alloying elements during the fabrication process, facilitating their incorporation into the TiAl alloy. While several alloying elements have been investigated, copper (Cu) has shown potential for improving the microstructural characteristics and mechanical properties of titanium alloys. Copper alloying can refine the grain structure of titanium alloys, leading to improved mechanical strength and ductility [11]. It has also been observed that copper can enhance the precipitation of secondary phases, such as Ti_2Cu and TiCu, which contribute to the strengthening mechanisms in the alloy [12]. Additionally, copper can promote the formation of a fine dispersion of intermetallic precipitates, which can further enhance the mechanical properties and thermal stability of titanium alloys [13].

Furthermore, copper alloying has been found to influence the phase transformation behavior of titanium alloys. The presence of copper can alter the materials' phase stability and kinetics, leading to modifications in the transformation temperatures and phase compositions. These changes can affect the microstructural evolution and mechanical properties of titanium alloys during processing and subsequent heat treatments [14].

Additionally, the microstructures of TiAl alloys can be further tailored by controlling the processing parameters during selective laser melting (SLM). Adjusting processing parameters can alter the heat input as well as thermal history of the material, leading to modifications of the composition and microstructure of the alloy. Multiple-scan strategies can be employed to locally modify the composition and microstructure of the TiAl alloy [15]. This approach allows for the creation of distinct microstructural regions within a single component, which can exhibit different properties suited to specific operating conditions. Specifically, by adjusting the aluminum (Al) content through multiple scans, it is possible to create Al-rich regions with a near-gamma microstructure for improved room-temperature ductility, and Al-lean regions with a lamellar microstructure for enhanced high-temperature properties, such as creep resistance [16].

Generally, TiAl alloys can exhibit four primary types of microstructures: fully lamellar (FL), nearly lamellar (NL), duplex, and near-gamma (NG) types. The FL microstructure consists of alternating lamellae of the α_2-Ti_3Al phase and the γ-TiAl phase, exhibiting excellent creep resistance and high-temperature strength. The NL microstructure, with a lower volume fraction of the lamellar α_2-Ti_3Al phase, offers a balance between high-temperature strength and room-temperature ductility. The duplex microstructure, comprising a mixture of lamellar α_2-Ti_3Al and equiaxed γ-TiAl phases, exhibits improved room-temperature ductility but reduced creep resistance compared to FL and NL microstructures. The NG microstructure, predominantly composed of the γ-TiAl phase with limited α_2-Ti_3Al phase, displays excellent room-temperature ductility but lower creep resistance [9,10]. The specific microstructure obtained in TiAl alloys depends on the heat treatment temperature relative to the alpha-transus temperature [17].

In this study, we aim to investigate the effect of in situ copper alloying on the microstructure of TiAl-based alloys fabricated using SLM, both in their as-fabricated state and after a subsequent heat treatment. Furthermore, we explore the impact of using multiple laser scans as an additional heat input to modify the microstructure and composition of TiAl intermetallic alloys, enabling the creation of dual microstructural designs suitable for different operating conditions. Through an analysis of the materials' microstructural changes, phase compositions, and mechanical properties, we seek to enhance the existing

methods for fabricating TiAl intermetallic alloys and pave the way for the development of advanced TiAl-based materials with properties tailored to diverse applications.

2. Materials and Methods

2.1. Powder Preparation

For the investigation of the effects of copper in situ alloying on the microstructure and properties of TiAl alloys, we used spherical gas-atomized powder of the TiAl alloy with a particle size distribution of 22.6–70.7 μm (d10–d90), a median particle size d50 = 39 μm, and a nominal composition of Ti-48Al-2Cr-2Nb-1.5V-0.1Gd (at. %), as shown in Figure 1a. Elemental copper powder with a dendritic particle shape and a median particle size of 37 μm was mixed with the TiAl alloy powder in a tumbler mixer for 12 h (Figure 1c). Powder mixtures with different copper contents were prepared: TiAl-0Cu, TiAl-2Cu, TiAl-4Cu, and TiAl-6Cu, corresponding to 0, 2, 4, and 6 wt.% of copper, respectively.

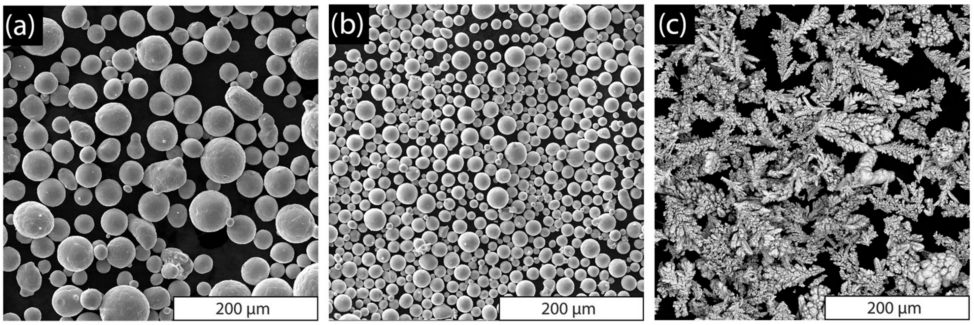

Figure 1. Powder materials used in the investigation: (**a**) Ti-48Al-2Cr-2Nb-1.5V-0.1Gd (at. %) powder, (**b**) Ti-48Al-2Cr-2Nb powder, (**c**) copper powder.

For the investigation of the potential of using multiple laser scans to tailor the microstructures of TiAl alloys in the SLM process, we utilized the gas-atomized powder of the Ti-48Al-2Cr-2Nb (at. %) alloy (Ti4822) from AMC Powders, Beijing, China. The powder had a particle size d10 = 17.4 μm, d90 = 60.5 μm, and a median particle size d50 = 33.8 μm (Figure 1b).

2.2. Selective Laser Melting (SLM) Process

The AconityMIDI (Aconity3D GmbH, Herzogenrath, Germany) SLM system equipped with a 1000 W fiber laser with a wavelength of 1060 nm was used to fabricate the bulk samples. To mitigate cracking issues during the SLM process, an inductive heating element was employed to preheat a titanium substrate to 900 °C. The process chamber was purged with Argon gas during the SLM process. The following SLM process parameters were used: a laser power of 230 W, a scanning speed of 800 mm/s, a hatching distance of 120 μm, and a layer thickness of 50 μm.

Multiple laser scans were utilized to modify the composition and microstructure of the TiAl alloy. Samples labeled X1 were produced using a single laser scan per layer. Additional laser scanning was performed for samples labeled X10, where each layer was scanned ten times. The parameters for the additional scanning were as follows: a laser power of 230 W, a scanning speed of 1400 mm/s, and a hatching distance of 300 μm.

2.3. Analysis of Microstructures and Phase Composition

Polished sections of the fabricated specimens were studied using a Mira 3 scanning electron microscope (SEM) in the backscattered electrons (BSE) mode (TESCAN, Brno, Czech Republic). The microstructure of the samples was analyzed using the SEM.

The phase composition of the samples was analyzed using a Bruker D8 Advance X-ray diffraction (XRD) meter (Bruker, Bremen, Germany) with Cu-Kα (λ = 1.5418 Å) irradiation. The XRD analysis provided information about the phase composition of the TiAl alloys.

2.4. Tensile and Compressive Testing

Tensile and compressive tests were performed using a Z100 testing machine (Zwick/Roell, Ulm, Germany). The tensile direction was perpendicular to the build direction (BD) of the samples. Three tensile and compressive samples per point were tested to evaluate the average values of the mechanical properties.

2.5. Heat Treatment

Heat treatment was carried out using a Carbolite vacuum furnace (Carbolite Gero, Neuhausen, Germany) with a 10 °C/min heating rate and a 2 h soaking time, followed by furnace cooling. Two annealing temperatures were used: (1) below the α-transus (or γ-solvus) temperature at 1260 °C; (2) above the α-transus temperature at 1350 °C in the single α-phase region.

2.6. Microhardness Testing

The microhardness testing of the samples was carried out using the VH1150 testing machine (VH1150, Buehler, Chicago, IL, USA) with a Vickers indenter at a 500 g load and a 10 s dwell time. At least five measurements were taken at a randomized position for each sample.

3. Results

3.1. Copper's Influence on the Microstructure and Mechanical Properties of TiAl Alloys

The initial microstructure obtained after the SLM process predominantly consists of homogeneous TiAl with evenly distributed precipitates of gadolinium oxide Gd_2O_3. The introduction of copper into the alloy leads to the formation of α_2-Ti_3Al and an increase in its volume fraction with the increase in the Cu content (Figure 2c). In the case of the addition of 6 wt.% Cu, the microstructure consists of lamellar Ti_3Al colonies surrounded by γ-phase boundaries (Figure 2d).

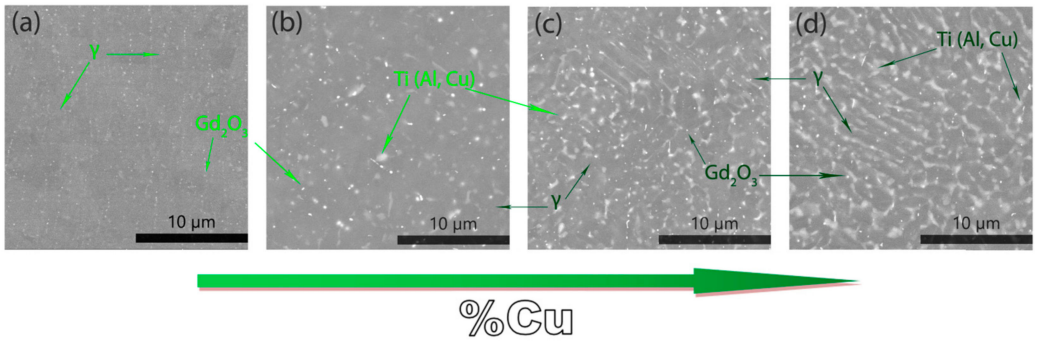

Figure 2. SEM microstructure images of TiAl alloy samples with (**a**) 0, (**b**) 2, (**c**) 4, and (**d**) 6 wt.% Cu content.

The results of the XRD analysis shown in Figure 3 indicate that the obtained samples consist of a TiAl phase with a weakly expressed β-phase body-centered cubic Ti-lattice and an α_2 phase (Ti_3Al), which is similar to the as-SLMed TiAl alloy obtained without copper alloying. A β-phase formation can be caused by the modifiers Cr, Nb, and V, which are part of the TiAl-Cu alloy, stabilizing the bcc lattice β phase [16]. Increasing the copper content to 4 wt.% leads to the formation of a Cu-rich intermetallic phase based on Ti and Al compounds.

Figure 4 presents BSE-SEM images that reveal the different effects on the Ti-48Al-2Cr-2Nb-1.5V-0.1Gd (at. %) samples of 0, 2, 4, 6 wt.% Cu after heat treatment at 1260 °C. The sample without copper is represented by a mixed fine-grained microstructure consisting of Ti_3Al regions and a uniformly distributed precipitated γ phase. This phase composition is preserved along with gadolinium oxide precipitates, while an increase in the amount of copper in the alloy is accompanied by grain growth and the thickening of the intergranular

γ-TiAl boundary. The most significant influence on grain growth appears when the copper content is 6 wt.%, with the achievement of a duplex γ/α_2 microstructure. The α_2-phase crystallites have an average size of 30 µm and a closed-to-equiaxed form. A copper-rich phase in the form of discontinuous particles is detected along the grain boundaries. It is assumed to be a non-equilibrium state of the Ti_2Cu compound, coexisting with the γ-TiAl phase.

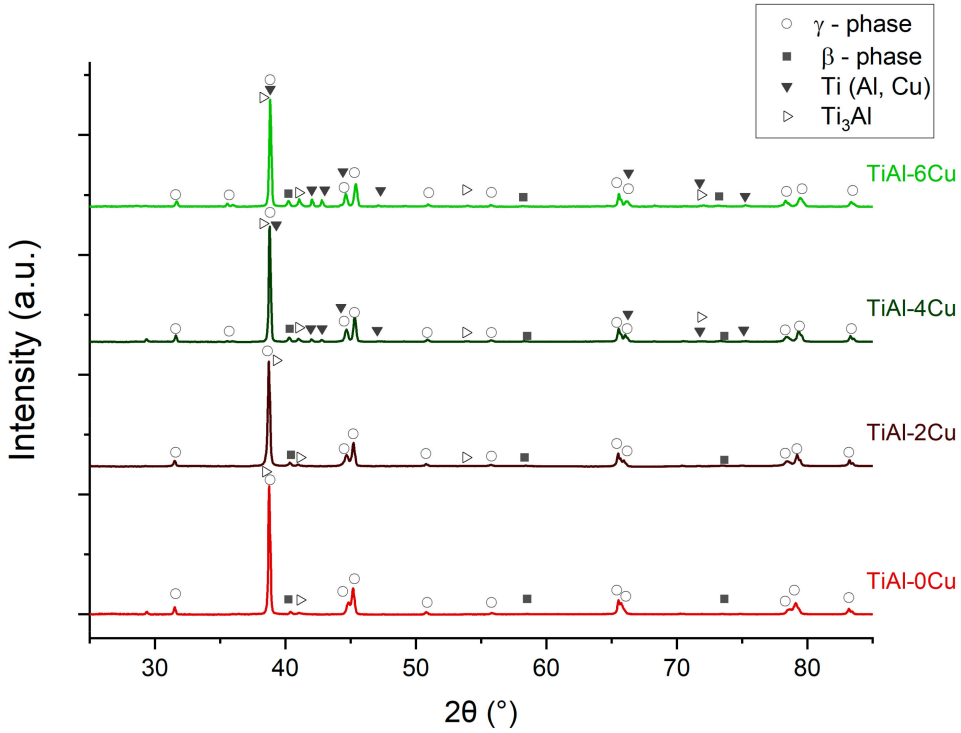

Figure 3. XRD results for the TiAl-Cu samples with different copper content.

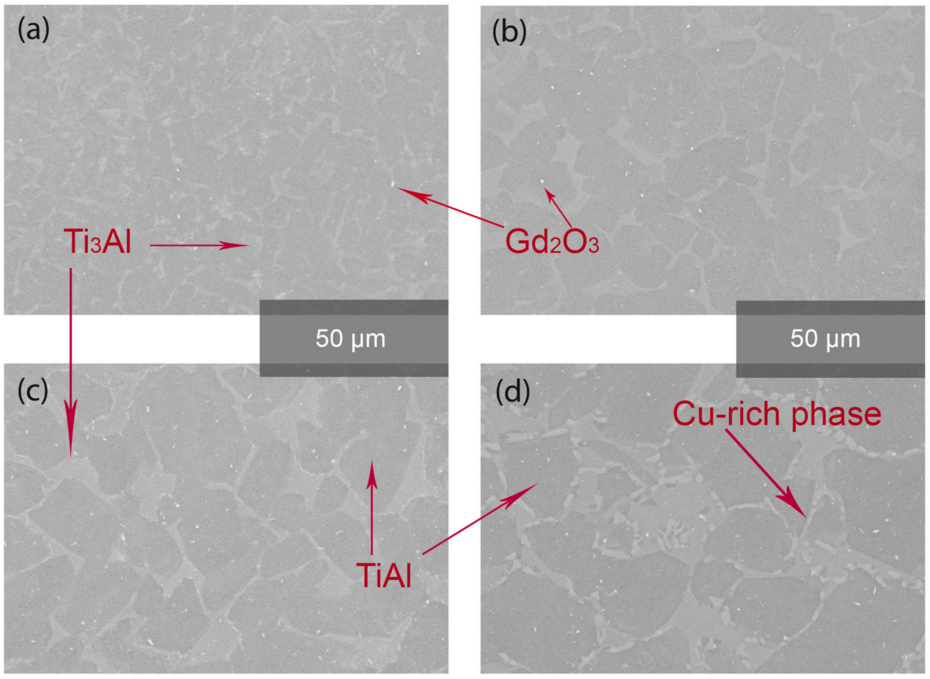

Figure 4. BSE-SEM images showing the microstructure of the Ti-48Al-2Cr-2Nb-1.5V-0.1Gd (at. %) alloy samples fabricated using SLM in situ alloying with (**a**) 0, (**b**) 2, (**c**) 4, and (**d**) 6 wt.% Cu after annealing at 1260 °C.

Figure 5 shows the variation in the TiAl alloy sample's microhardness with differing Cu content. The heat treatment resulted in a significant increase in the Ti-48Al-2Cr-2Nb-1.5V-0.1Gd (at. %) alloy's hardness, with the highest alloying efficiency being observed both for a copper content of 6 wt.%, and for annealing at 1250 °C without copper content. The decrease in microhardness after annealing can be attributed to grain growth and the formation of coarse precipitates.

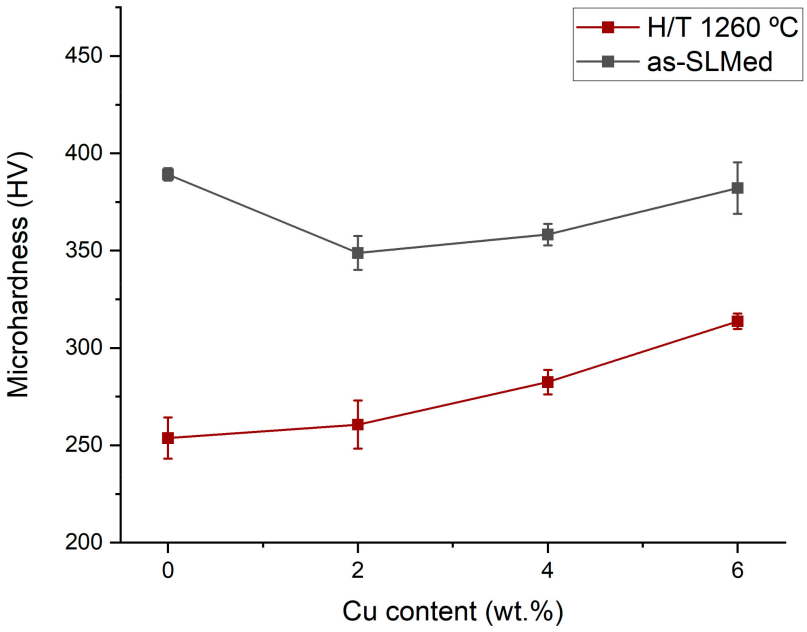

Figure 5. Microhardness of TiAl alloys with 0, 2, 4, and 6 wt.% Cu content in their initial state and after annealing.

Table 1 shows the results of the tensile tests of the TiAl-Cu samples. The most effective strength effect is observed in the TiAl-4Cu samples (Table 1), which, according to the XRD shown in Figure 3, reveals Ti (Cu, Al)-phase incipience and an increase in the α_2-Ti_3Al phase volume fraction. This confirms the previously obtained data on the strengthening effect of the α_2 phase in titanium aluminide alloys [18,19]. The strengthening effect of Ti_3Al with 6 wt.% Cu may be weakened by the presence of enlarged Cu-rich precipitates, which are formed along the grain boundaries. Along with this, heat treatment at 1260 °C of the as-SLMed TiAl-6Cu sample significantly reduces the tensile strength to 154 MPa.

Table 1. Tensile strength of TiAl samples with 0, 2, 4, and 6 wt.% Cu content.

Copper Content	0 wt.%Cu	2 wt.%Cu	4 wt.%Cu	6 wt.%Cu
Tensile strength, MPa	210 ± 15	276 ± 25	432 ± 25	256 ± 16

3.2. The Influence of the Multiple Scans on the Microstructure and Mechanical Properties of Ti4822 Alloys

The microstructures of the Ti4822 alloy samples, obtained as a result of multiple laser scans, as well as after annealing at 1260 °C and 1350 °C, are shown in Figure 6. The BSE-SEM images revealed the transformation of the as-fabricated homogeneous near-lamellar γ/α_2 phase microstructure with fine oxide inclusions in the near-globular microstructure after 1260 °C annealing.

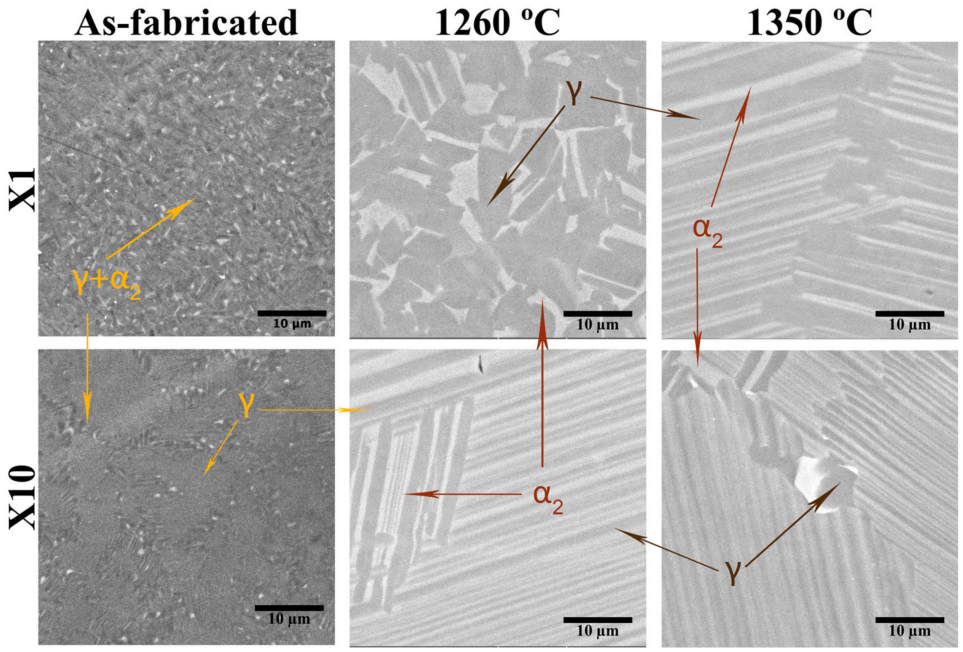

Figure 6. BSE-SEM images showing the microstructures of the TiAl alloy samples obtained using single-scan (X1) and multiple-laser-scan strategies in their as-fabricated states, as well as after annealing at 1260 °C and 1350 °C (dark areas represent the γ (TiAl) phase, and light areas represent the α_2 (Ti_3Al) phase).

This significantly differs from the lamellar-type microstructure, which was obtained in the X10 sample using the ten-scan strategy and subsequent annealing at the same temperature (1260 °C). The initial fine duplex [16] microstructure with γ-grains transformed into the near-lamellar microstructure.

Heat treatment of the Ti4822 alloy at 1350 °C after a single scan resulted in the fully lamellar microstructure. In the case of the Ti4822 alloy obtained using multiple laser scans, lamellar colonies mixed with near-globular grains were found.

Heat treatment in the β region at 1350 °C after SLM with the multiple-scan strategy leads to the formation of a mixed nearly lamellar γ + α_2 coarse microstructure (Figure 6), with mixed duplex emissions formed on the grain boundaries.

The results of the XRD analysis, shown in Figure 7, indicate the presence of a predominant γ-TiAl phase. Annealing at 1260 °C had no significant effect on the change in the diffraction pattern of the Ti4822 alloy obtained using a single laser scan. Annealing at 1350 °C led to the redistribution of the α_2/γ phase ratio in the direction of the decreasing fraction of the γ-TiAl phase. Using multiple laser scans resulted in the increased volume fraction of the α_2 phase.

Figure 8 shows the results of compressive tests for the Ti4822 alloy samples fabricated using single (X1)- and multiple (X10)-laser-scan strategies before and after annealing. The comparison shows an insignificant change in the tensile strength of the Ti4822 alloy after heat treatment at 1260 °C and significant decreases in the compressive strength, by 20%, and compressive strain, by 18%, as a result of annealing at 1350 °C for the samples that were obtained by both the single- and multiple-scan strategies. Multiple laser scans resulted in decreases in the compressive strength (11%) and compressive strain (15%). The highest compressive strain of 34.4% and highest compressive strength of 1740 MPa were obtained for the X1 samples after annealing at 1260 °C. It is worth noting that the lamellar microstructure obtained in the X10 sample after annealing at 1260 °C supposedly exhibits better creep resistance than the as-SLMed duplex microstructure. The demonstrated possibility of achieving different types of microstructures after annealing by varying the scanning strategy can be further explored to locally tailor the microstructure in a particular part of the

material by creating functionally graded microstructures for locally optimized mechanical performance.

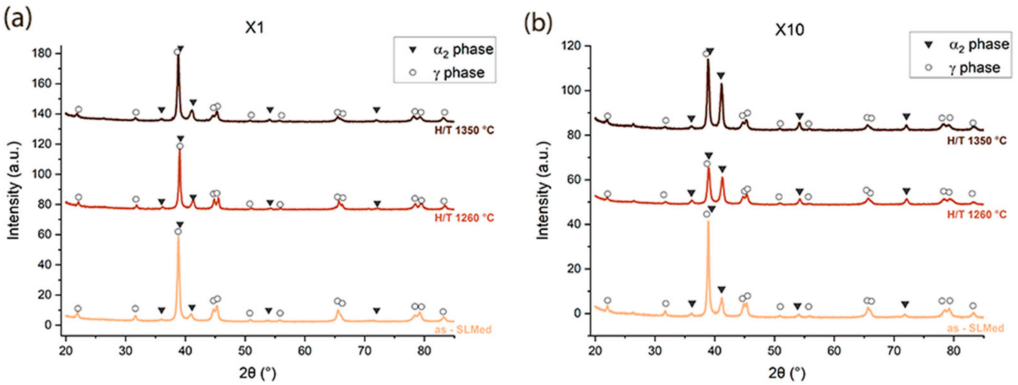

Figure 7. XRD results of the Ti4822 samples obtained using SLM with different scanning strategies and after annealing at 1260 °C and 1350 °C: (**a**) X1—single scan; (**b**) X10—multiple scans (10 times).

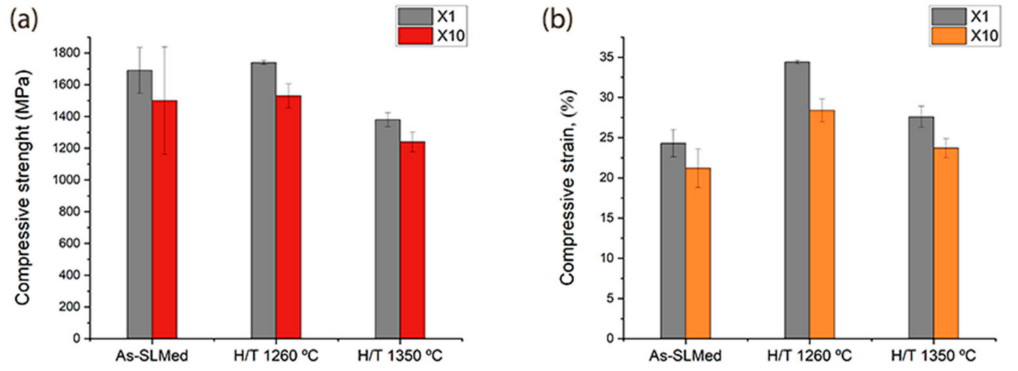

Figure 8. Compression test results of the Ti4822 alloy samples obtained using SLM with different scanning strategies and after annealing: (**a**) compressive strength and (**b**) compressive strain.

4. Discussion

4.1. Copper's Influence on the Microstructure of the TiAl Alloy

The addition of copper (Cu) to the beta stabilizers present in the TiAl alloy, such as niobium (Nb) and chromium (Cr), plays a crucial role in modifying the material's microstructure and mechanical properties. It can suppress the eutectoid decomposition $\alpha \rightarrow \gamma + \alpha_2$. The initial microstructure obtained after the selective laser melting (SLM) process predominantly consists of homogeneous TiAl with evenly distributed precipitates of gadolinium oxide (Gd_2O_3). However, with the introduction of copper into the alloy, a notable transformation occurs. The α_2-Ti_3Al phase begins to form, and its volume fraction increases with the content of Cu (Figure 2c). Notably, when 6 wt.% of Cu is added to the alloy, the microstructure evolves into lamellar Ti_3Al colonies surrounded by γ-phase boundaries (Figure 2d). The low presence of the hexagonal α_2 phase, detected as a result of the XRD analysis of the TiAl-4Cu and TiAl-6Cu alloys, is accompanied by an intermediate metastable phase Ti (Al, Cu), the volume fraction of which is enhanced as the Cu content increases. The presence of an additional Cu-enriched phase is noted in the case of the compacting and subsequent liquid-phase sintering at 1375 °C for 120 min of the Ti4822 alloy powder, while the hexagonal close-packed phase is also saturated with Cr [20]. The X-ray diffraction (XRD) analysis (Figure 3) further supports these findings, indicating that the obtained samples consist of a TiAl phase with a weakly expressed body-centered cubic (bcc) β phase of the Ti-lattice and an α_2 phase (Ti_3Al). The presence of the β phase can be attributed to the modifiers Cr, Nb, and V, which are part of the TiAl-Cu alloy and serve to stabilize the bcc lattice β phase [21]. As the copper content increases to 4 wt.%, a Cu-rich

intermetallic phase, based on Ti and Al compounds, is observed. This suggests that copper significantly influences the phase composition, and its presence may lead to the formation of new intermetallic compounds within the alloy.

Due to the fact that, in titanium alloys, copper appears as an eutectoid-forming component [13,22,23], phase Ti (Al, Cu) found as a result of the XRD study can be considered a precursor of the Ti_2Cu intermetallic compound. It also contributes to an increase in hardness after heat treatment, similarly to the eutectoid Ti_2Cu intermetallic compound [24].

Microstructure characterization through backscattered electron scanning electron microscopy (BSE-SEM) imaging (Figure 4) shows the effects of adding copper after heat treatment at 1260 °C. In the absence of copper, the microstructure consists of a mixed fine-grained morphology comprising Ti_3Al regions and a uniformly distributed precipitated γ phase. Notably, as the copper content increases, grain growth occurs, accompanied by intergranular γ-TiAl boundary thickening. At 6 wt.% Cu, a duplex γ/α_2 microstructure is achieved, where α_2-phase crystallites with an average size of 30 μm appear in a close-to-equiaxed form. Along the grain boundaries, discontinuous particles of the copper-rich phase, likely a non-equilibrium state of the Ti_2Cu compound, are detected. This observation underscores the complexity of the microstructural evolution resulting from the interplay of the Cu and TiAl phases during the heat treatment.

The tensile strength results (Table 1) provide further insights into the impact of copper content on the mechanical behavior of the TiAl samples. The TiAl-4Cu samples exhibit the most effective strengthening effect, as is consistent with the XRD findings of an increased α_2-Ti_3Al phase volume fraction. This strengthening effect can be attributed to the role of the α_2 phase in titanium aluminide alloys, which has been reported in previous studies [19]. Nevertheless, the tensile strength of TiAl with 6 wt.% Cu appears to be influenced by enlarged Cu-rich precipitates formed along the grain boundaries, resulting in reduced strength. Furthermore, heat treatment at 1260 °C significantly decreases the tensile strength of the as-SLMed TiAl-6Cu sample to 154 MPa. This emphasizes the importance of carefully tailoring the copper content to optimize the mechanical properties of TiAl alloys.

The hardening effect of copper alloying, in small amounts, can be useful for practical applications. However, exceeding 4 wt.% Cu tends to reduce the strength of the TiAl alloy [21]. This may be due to the formation of a brittle Ti (Al, Cu) phase along the grain boundaries; in this case, the accumulation of dislocations on the grain boundaries should be taken into account, as they contribute to the cracks' formation. This is also true for the increased grain size. These assumptions require confirmation with further investigations.

Additionally, exploring the influence of alloying elements other than copper on the microstructure and properties of TiAl alloys could present exciting avenues for alloy optimization. The interaction between various alloying elements and their combined effects on phase formation, grain structure, and mechanical properties deserves thorough investigation [22]. Furthermore, advanced characterization techniques, such as transmission electron microscopy (TEM), atom probe tomography (APT), and in situ mechanical testing, can provide valuable insights into the underlying mechanisms governing the behavior of copper-alloyed TiAl alloys.

4.2. The Influence of Repeating Scanning on the Microstructures of the Ti4822 Alloys

The use of the multiple-laser-scan strategy makes it possible not only to form a controlled microstructure, but also to manage the chemical composition. According to the EDX (energy dispersive X-ray) analysis, the Al content in the alloy is reduced by 2.7 at. % after X1 scanning and by 6 at.% after the X10 scanning strategy compared to the nominal composition of the feedstock powder (Figure 9). The Al content is reduced down to 42.5 at. % due to high-temperature evaporation, while the content of other elements is almost fully consistent (Table 2). This is reflected in the near-γ microstructure consisting of equiaxed γ-phase grains with a finely lamellar α_2/γ phase distributed along the grain boundaries. After heat treatment at 1250 °C, the Ti4822 alloy with reduced Al content exhibits a fully lamellar microstructure.

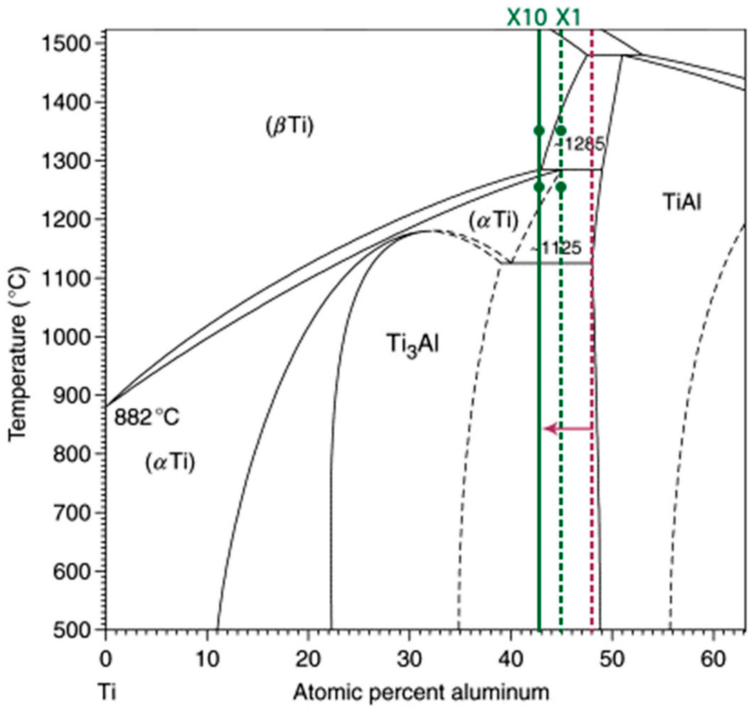

Figure 9. Ti-Al phase diagram showing the Al content obtained in the Ti4822 alloy samples using the X1 and X10 scanning strategies.

Table 2. EDX results showing the chemical composition of the Ti4822 alloy samples obtained by SLM with the single-scan (X1) and multiple-scan (X10) strategies.

Element Content, at. %	Ti	Al	Cr	Nb
Feedstock powder nominal composition	48	48	2	2
X1 scanning	50.54	45.26	2.12	2.07
X10 scanning	52.91	42.49	1.95	2.65

According to the phase diagram, the phase composition obtained as a result of applying various scanning strategies in all cases causes the alloy to undergo the peritectoid decomposition of α-Ti, which goes via the α_2 (Ti_3Al) + γ two-phase region with different α_2 to γ phase ratios [24]. Thereafter, the XRD results for the X10 sample demonstrate increased peaks of the α_2 phase, which is a Ti_3Al intermetallic compound that requires less Al to form compared to the TiAl intermetallic compound. Moreover, the XRD results do not show any β-phase peaks for the X10 sample after heat treatment at 1350 °C.

Cooling from the β-phase region in alloys, with the presence of a strong beta stabilizer Nb and Cr, proceeds with the formation of an ordered derivative of the β-phase–B2-phase, located along the coarse lamellar γ grains (the white regions in Figure 6.) [19,25].

Phase transformations occurring in the alloy, obtained by SLM with multiple scanning and heat treatment at 1350 °C, follow the pathway: β → (β + α) → α → lamellar (γ/α_2), while the transformation β/B2 → γ, leading to the formation of an α_2 + β + γ mixture along the lamellar colonies, also comes from the nonequilibrium state of the alloy as a result of high cooling rates during laser remelting. Similar transformations have been described for cast and hot-worked TiAl alloys [26,27]. The presence of the β phase is considered undesirable from the point of view of ensuring the ductility and workability of the alloy at room temperature due to the higher hardness of the β phase compared to the α_2 and γ phases [26,28]. At the same time, the presence of β precipitates worsens the compressive strain and is able to contribute to creep resistance. Thus, the samples obtained after SLM with single and multiple scans and heat treatment at 1350 °C exhibit more balanced properties that are suitable for machining [29,30].

The heat treatment at 1350 °C preceding alpha decomposition in the β phase region leads to the formation of the supposed B2 modification of the metastable β phase on the triple points and the grain boundaries. The formation of a mixed γ(TiAl)+β phase structure in the intergranular space presumably leads to a deterioration in the strength and plastic properties of the alloy due to the negative effect of the brittle low-temperature β_0 phase [28,31].

5. Conclusions

This study investigated the influence of in situ copper alloying and multiple laser scanning on the microstructure and mechanical properties of TiAl-based alloys fabricated using selective laser melting (SLM). The following conclusions can be drawn from the experimental results:

1. Copper alloying enhances the formation of the α_2-Ti_3Al phase and increases its volume fraction in TiAl alloys. The addition of copper refines the material's microstructure, leading to the formation of lamellar colonies surrounded by γ-phase boundaries.
2. The microstructural changes induced by copper alloying result in improved mechanical properties. TiAl alloys with added copper exhibited higher microhardness and tensile strength compared to the alloy without copper. The TiAl-4Cu composition showed the highest tensile strength (432 ± 25 MPa) among the investigated compositions.
3. Heat treatment of the TiAl-Cu alloys at 1260 °C led to grain growth, intergranular γ-TiAl boundary thickening, and the formation of coarse Cu-rich intermetallic phases. This heat treatment also reduced the tensile strength and ductility of the alloys.
4. The use of multiple laser scans during the SLM process allows for the creation of tailored microstructures. The use of the single- and multiple-scan strategies resulted in different microstructural designs, such as near-lamellar and lamellar structures. Heat treatments at different temperatures further modified the microstructures, leading to fully lamellar or mixed nearly lamellar γ + α structures.
5. The mechanical properties of the TiAl alloys were affected by the microstructural changes induced by the multiple laser scans and heat treatment. The samples with near-lamellar microstructures exhibited higher compressive strength and strain compared to the samples with fully lamellar or mixed structures.

Author Contributions: Conceptualization, I.P. and V.S.; formal analysis, A.G.; funding acquisition, A.P.; investigation, V.S. and A.G.; methodology, I.P.; project administration, A.P.; supervision, I.P.; visualization, A.G.; writing—original draft, V.S.; writing—review and editing, I.P. and A.P. All authors have read and agreed to the published version of the manuscript.

Funding: The research was supported by the Russian Science Foundation, grant No. 23-79-30004, https://rscf.ru/project/23-79-30004/ (accessed on 12 July 2023).

Data Availability Statement: The data presented in this study are available on request from the corresponding author.

Conflicts of Interest: The authors declare no conflict of interest.

References

1. Soliman, H.A.; Elbestawi, M. Titanium aluminides processing by additive manufacturing—A review. *Int. J. Adv. Manuf. Technol.* **2022**, *119*, 5583–5614. [CrossRef]
2. Vogelpoth, A.; Schleifenbaum, J.H.; Rittinghaus, S. Laser Additive Manufacturing of Titanium Aluminides for Turbomachinery Applications. In Proceedings of the ASME Turbo Expo 2019: Turbomachinery Technical Conference and Exposition, Phoenix, AZ, USA, 17–21 June 2019; Volume 6. [CrossRef]
3. Mallikarjuna, B.; Reutzel, E.W. Reclamation of intermetallic titanium aluminide aero-engine components using directed energy deposition technology. *Manuf. Rev.* **2022**, *9*, 27. [CrossRef]

4. Duan, B.; Yang, Y.; He, S.; Feng, Q.; Mao, L.; Zhang, X.; Jiao, L.; Lu, X.; Chen, G.; Li, C. History and development of γ-TiAl alloys and the effect of alloying elements on their phase transformations. *J. Alloys Compd.* **2022**, *909*, 164811. [CrossRef]
5. Yang, X.; Zhang, B.; Bai, Q.; Xie, G. Correlation of microstructure and mechanical properties of Ti_2AlNb manufactured by SLM and heat treatment. *Intermetallics* **2021**, *139*, 107367. [CrossRef]
6. Polozov, I.; Sufiiarov, V.; Kantyukov, A.; Razumov, N.; Goncharov, I.; Makhmutov, T.; Silin, A.; Kim, A.; Starikov, K.; Shamshurin, A.; et al. Microstructure, densification, and mechanical properties of titanium intermetallic alloy manufactured by laser powder bed fusion additive manufacturing with high-temperature preheating using gas atomized and mechanically alloyed plasma spheroidized powders. *Addit. Manuf.* **2020**, *34*, 101374. [CrossRef]
7. Polozov, I.; Kantyukov, A.; Goncharov, I.; Razumov, N.; Silin, A.; Popovich, V.; Zhu, J.-N.; Popovich, A. Additive Manufacturing of Ti-48Al-2Cr-2Nb Alloy Using Gas Atomized and Mechanically Alloyed Plasma Spheroidized Powders. *Materials* **2020**, *13*, 3952. [CrossRef] [PubMed]
8. Wang, J.; Luo, Q.; Wang, H.; Wu, Y.; Cheng, X.; Tang, H. Microstructure characteristics and failure mechanisms of Ti-48Al-2Nb-2Cr titanium aluminide intermetallic alloy fabricated by directed energy deposition technique. *Addit. Manuf.* **2019**, *32*, 101007. [CrossRef]
9. Genc, O.; Unal, R. Development of gamma titanium aluminide (γ-TiAl) alloys: A review. *J. Alloys Compd.* **2022**, *929*, 167262. [CrossRef]
10. Polozov, I.; Gracheva, A.; Popovich, A. Processing, Microstructure, and Mechanical Properties of Laser Additive Manufactured Ti_2AlNb-Based Alloy with Carbon, Boron, and Yttrium Microalloying. *Metals* **2022**, *12*, 1304. [CrossRef]
11. Wang, Q.; Zhang, K.; Niu, W. Microstructural characteristic and mechanical properties of titanium-copper alloys in-situ fabricated by selective laser melting. *J. Alloys Compd.* **2021**, *885*, 161032. [CrossRef]
12. Akbarpour, M.R.; Mirabad, H.M.; Hemmati, A.; Kim, H.S. Processing and microstructure of Ti-Cu binary alloys: A comprehensive review. *Prog. Mater. Sci.* **2022**, *127*, 100933. [CrossRef]
13. Cardoso, F.; Cremasco, A.; Contieri, R.; Lopes, E.; Afonso, C.; Caram, R. Hexagonal martensite decomposition and phase precipitation in Ti–Cu alloys. *Mater. Des.* **2011**, *32*, 4608–4613. [CrossRef]
14. Vilardell, A.M.; Yadroitsev, I.; Yadroitsava, I.; Albu, M.; Takata, N.; Kobashi, M.; Krakhmalev, P.; Kouprianoff, D.; Kothleitner, G.; du Plessis, A. Manufacturing and characterization of in-situ alloyed Ti6Al4V(ELI)-3 at.% Cu by laser powder bed fusion. *Addit. Manuf.* **2020**, *36*, 101436. [CrossRef]
15. Wartbichler, R.; Clemens, H.; Mayer, S. Electron Beam Melting of a β-Solidifying Intermetallic Titanium Aluminide Alloy. *Adv. Eng. Mater.* **2019**, *21*, 1900800. [CrossRef]
16. Mphahlele, M.; Olevsky, E.; Olubambi, P. Chapter 12-Spark plasma sintering of near net shape titanium aluminide: A review. In *Spark Plasma Sintering*; Elsevier: Amsterdam, The Netherlands, 2019; pp. 281–299. [CrossRef]
17. Leyens, C.; Peters, M. *Titanium and Titanium Alloys. Fundamentals and Applications*; Wiley-VCH: Weinheim, Germany, 2006; ISBN 3527305343.
18. Sun, F.-S.; Cao, C.-X.; Yan, M.-G.; Kim, S.-E.; Tailee, Y. Alloying mechanism of beta stabilizers in a TiAl alloy. *Metall. Mater. Trans. A Phys. Metall. Mater. Sci.* **2001**, *32*, 1573–1589. [CrossRef]
19. Raji, S.A.; Popoola, A.P.I.; Pityana, S.L.; Popoola, O.M. Characteristic effects of alloying elements on β solidifying titanium aluminides: A review. *Heliyon* **2020**, *6*, e04463. [CrossRef] [PubMed]
20. Xia, Y.; Luo, S.D.; Wu, X.; Schaffer, G.B.; Qian, M. The sintering densification, microstructure and mechanical properties of gamma Ti–48Al–2Cr–2Nb alloy with a small addition of copper. *Mater. Sci. Eng. A* **2013**, *559*, 293–300. [CrossRef]
21. Huang, X.-M.; Zhang, S.-X.; Cai, G.-M.; Liu, H.-S. Study on the evolution of phase relations in the Ti–Al–Nb/Cr systems at 0–50 at.% Al region. *Calphad* **2022**, *79*, 102461. [CrossRef]
22. Ju, J.; Zan, R.; Shen, Z.; Wang, C.; Peng, P.; Wang, J.; Sun, B.; Xiao, B.; Li, Q.; Liu, S.; et al. Remarkable bioactivity, bio-tribological, antibacterial, and anti-corrosion properties in a Ti-6Al-4V-xCu alloy by laser powder bed fusion for superior biomedical implant applications. *Chem. Eng. J.* **2023**, *471*, 144656. [CrossRef]
23. Xu, Y.; Jiang, J.; Yang, Z.; Zhao, Q.; Chen, Y.; Zhao, Y. The Effect of Copper Content on the Mechanical and Tribological Properties of Hypo-, Hyper- and Eutectoid Ti-Cu Alloys. *Materials* **2020**, *13*, 3411. [CrossRef]
24. Clemens, H.; Mayer, S. Design, Processing, Microstructure, Properties, and Applications of Advanced Intermetallic TiAl Alloys. *Adv. Eng. Mater.* **2012**, *15*, 191–215. [CrossRef]
25. Song, L.; Xu, X.; You, L.; Liang, Y.; Lin, J. Phase transformation and decomposition mechanisms of the β (ω) phase in cast high Nb containing TiAl alloy. *J. Alloys Compd.* **2014**, *616*, 483–491. [CrossRef]
26. Niu, H.; Chen, Y.; Xiao, S.; Xu, L. Microstructure evolution and mechanical properties of a novel beta γ-TiAl alloy. *Intermetallics* **2012**, *31*, 225–231. [CrossRef]
27. Takeyama, M.; Kobayashi, S. Physical metallurgy for wrought gamma titanium aluminides: Microstructure control through phase transformations. *Intermetallics* **2005**, *13*, 993–999. [CrossRef]
28. Cui, N.; Wu, Q.; Yan, Z.; Zhou, H.; Wang, X. The Microstructural Evolution, Tensile Properties, and Phase Hardness of a TiAl Alloy with a High Content of the β Phase. *Materials* **2019**, *12*, 2757. [CrossRef]
29. Wang, J.; Nieh, T. Creep of a beta phase-containing TiAl alloy. *Intermetallics* **2000**, *8*, 737–748. [CrossRef]

30. Xia, Z.; Shan, C.; Zhang, M.; Cui, M.; Luo, M. Machinability of γ-TiAl: A review. *Chin. J. Aeronaut.* **2023**, *36*, 40–75. [CrossRef]
31. Schloffer, M.; Iqbal, F.; Gabrisch, H.; Schwaighofer, E.; Schimansky, F.-P.; Mayer, S.; Stark, A.; Lippmann, T.; Göken, M.; Pyczak, F.; et al. Microstructure development and hardness of a powder metallurgical multi phase γ-TiAl based alloy. *Intermetallics* **2012**, *22*, 231–240. [CrossRef]